**Proceedings of the ASME 2020 15th International Manufacturing Science and Engineering Conference**
**MSEC2020**
**June 22-26, 2020, Cincinnati, OH, USA**

**MSEC2020-8485**

# STUDY OF EFFECT OF REPETITION RATE ON LASER SHOCK PEENING USING FINITE ELEMENT MODELING

**Sai Kosaraju, and Xin Zhao.**
Department of Mechanical Engineering, Clemson University, Clemson, SC, USA

## ABSTRACT

*A two-dimensional finite element model is developed to simulate the interaction between metal samples and laser-induced shock waves. Multiple laser impacts are applied at each location to increase plastically affected depth and compressive stress. The in-depth and surface residual stress profiles are analyzed at various repetition rates and spot sizes. It is found that the residual stress is not sensitive to repetition rate until it reaches a very high level. At extremely high repetition rate (100 MHz), the delay between two shock waves is even shorter than their duration, and there will be shock wave superposition. It is revealed that the interaction of metal with shock wave is significantly different, leading to a different residual stress profile. Stronger residual stress with deeper distribution will be obtained comparing with lower repetition rate cases. The effect of repetition rate at different spot sizes is also studied. It is found that with larger laser spot, the peak compressive residual stress decreases but the distribution is deeper at extremely high repetition rates.*

Keywords: Laser shock peening, repetition rate, finite element modeling

## 1. INTRODUCTION

Laser shock peening is a cold working process which is used to improve material properties like surface hardness, fatigue life, wear and corrosion resistance, etc. [1, 2, 3]. It is widely used to treat turbines, fans, compressor blades, aircraft and automotive parts. When the material is irradiated by high power density laser pulses, shock waves are generated, which plastically deform the material surface and induce high compressive stresses within subsurface area. The amount of residual compressive stress and plastically affected depth depend on laser parameters (laser power density [4, 8, 9], pulse duration [8], wavelength [7], spot size [3, 4, 8, 9] and shape [4, 5]), materials, ambient environment, etc. To improve the application of laser shock peening, it is of critical importance to optimize the process by fully understanding the effects of different parameters. Extensive studies have been devoted to this area. Previous studies have demonstrated the benefit of using multiple shocks at the same location to increase the magnitude and depth of residual stresses. But the effect of time interval between successive spots which is determined by repetition rate has not been studied yet. Recently, thanks to the advance of laser technology, high repetition rate lasers could significantly improve this technique by increasing compressive residual stress and plastically affected depth. This research studies the effect of laser repetition rate at different spot sizes on the final shock peening results such as peak residual stress and plastically affected depth by finite element modeling.

## 2. RESIDUAL STRESS GENERATION

The propagation of shock waves through the metal causes it to deform plastically when the pressure of shock wave is greater than Hugoniot limit of the material [1, 2, 3]. Hugoniot elastic limit is the maximum stress a material can withstand in uniaxial direction without undergoing plastic deformation.

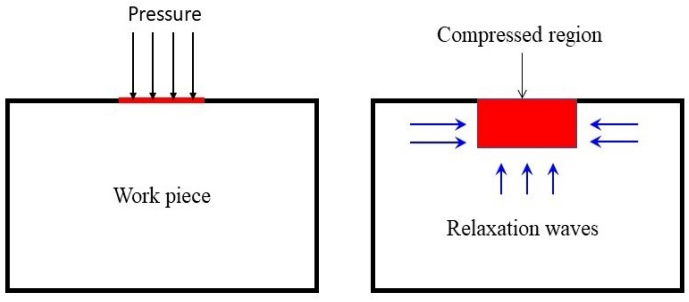


(a) Pressure input (b) Origin of relaxation waves
Figure 1. Generation of residual stress

Figure 1(a) and (b) show the effect of shock waves on the material. The top layers of the material under the influence of shock wave expand plastically. The expansion of material decreases with increase in depth and finally becomes zero. The tensile plastic deformation of the surface layers induces compressive residual stress which decreases with increase in depth. The expanded layers try to push away the material surrounding it inducing compressive plastic deformation. The residual stress becomes tensile around the affected area because of the compressive plastic deformation [4].

Figure 2 shows the variation of residual stress in depth direction for 1mm spot diameter. It varies from -426.08MPa to 82.85MPa. The peak value of tensile stress is less than peak value of compressive stress. But the volume of material in tensile state is greater than the volume in compressive state to attain equilibrium in the workpiece.

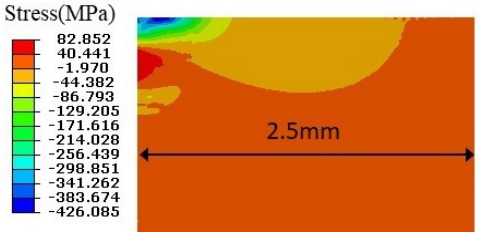


Figure 2. Residual stress distribution along depth for 1mm spot size predicted using axe-symmetric model.

After the pressure is removed, the relaxation waves generated at the boundary of affected area causes reverse straining, resulting in a decrease in residual stress [3, 5, 6, 7]. The reverse straining is more in the top layers of the material because of the free degree of freedom in z-direction. It causes stress hole at the center of circular spot because of the concentration of relaxation waves. This effect is less for square or rectangular spot shapes because of the absence of concentration of relaxation waves [5]. High magnitude and long duration of pressure pulses also increases the strength of relaxation waves. This is because of the increase in deformation of the material which generates stronger opposition from the boundary of the spot.

## 3. LASER REPETITION RATE

Material is subjected to multiple laser shots at the same location to increase peak compressive stress and plastically affected depth [2, 3, 8, 9, 10, 11, 12, 13]. The time interval between successive laser spots is determined by the repetition rate. Due to recent developments, lasers with very high repetition rates of 100 MHz have been developed, which open new possibilities of LSP by introducing completely different pressure-material interaction dynamics.

The effect of repetition rate is studied at 0.1 MHz, 1 MHz, 10 MHz and 100 MHz for spot diameters of 1 mm, 100 µm and 10 µm. The repetition rate can be characterized into three regimes. It takes about $10^{-5}$ s for the material to relax completely after irradiation of single laser pulse [4]. Therefore, repetition rates below 0.1 MHz can be considered to be the low repetition rate regime, where the material is completely relaxed between two successive pressure pulses. It is only partially relaxed at higher repetition rates. As shown in Figure 5, the pressure load introduced by a laser pulse can last for 50 ns, and thus there is no overlap of consecutive pressure pulses for repetition rates lower than 20 MHz. The pressure profile changes due to the overlap of consecutive pulses at repetition rates higher than 20 MHz, which is considered as the high repetition rate regime. For repetition rate of 100 MHz, the peak pressure is 1.6 times of that by a single pressure pulse. The repetition rate regime in between is the moderate regime.

To study the effect of pressure pulse overlap, repetition rates of 20 MHz and 33.3 MHz are used. The pressure pulses are applied one after the other without allowing the material to relax between successive spots at a repetition rate of 20 MHz. The overlap between successive pressure pulses does not change the peak pressure at 33.3 MHz. Repetition rates of 142.9 MHz and 200 MHz are also studied to check for the extent of change in plastically affected depth after 100 MHz.

Figure 3 and Figure 4 show the overlap of pressure profiles at repetition rates of 33.3MHz and 100MHz respectively. It is assumed that the profile of the incoming pressure wave will not be affected by the former pulse and the material properties remain unchanged.

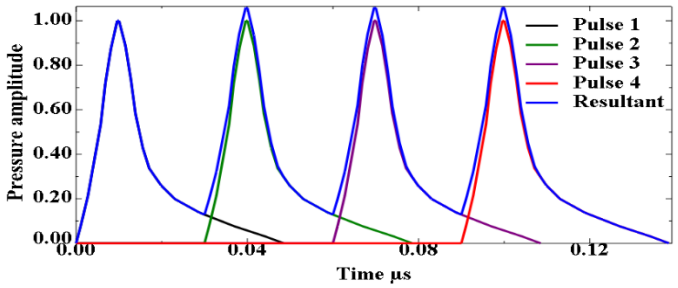


Figure 3. Overlap of pressure profiles at repetition rate of 33.3 MHz.

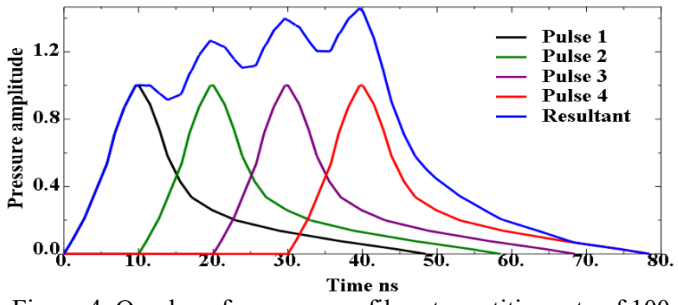


Figure 4. Overlap of pressure profiles at repetition rate of 100 MHz.

## 4. NUMERICAL MODEL

Since LSP is a fast process, it is difficult to experimentally study the propagation of shock wave and stress generation within the component at each time step. Therefore, a numerical model is needed to study the effect of input parameters and to optimize

them to increase peak compressive stresses and plastically affected depth.

The numerical model for LSP typically consists of two steps. In the first step, the laser material interaction is studied to determine the spatial and temporal pressure profiles induced into the sample. Extensive studies have been going on to determine the pressure profiles using models such as two-temperature model, hydrodynamic model etc. In the second step, the calculated pressure is applied as the surface load in the finite element model to obtain final residual stress profile in the material. This research focusses only on the second step since our aim is to study the effect of the laser repetition rate. The temporal pressure profile is borrowed from the conclusion of Ref. [14], where the laser parameters are pulse duration of 10 ns, pulse energy of 3 J and wavelength of 1064 nm, as shown in Figure 5 It raises to peak value in 10 ns and then gradually decreases. Based on this, the spatial pressure profile is calculated according to the Gaussian distribution:

$$P(r,t) = P(t)\exp\left(-\frac{r^2}{2R^2}\right) \qquad (1)$$

where P is the pressure, r is the distance from laser spot center, R is the laser spot radius, and x and y are coordinates of integration point. Figure 6 shows the Gaussian spatial distribution of pressure.

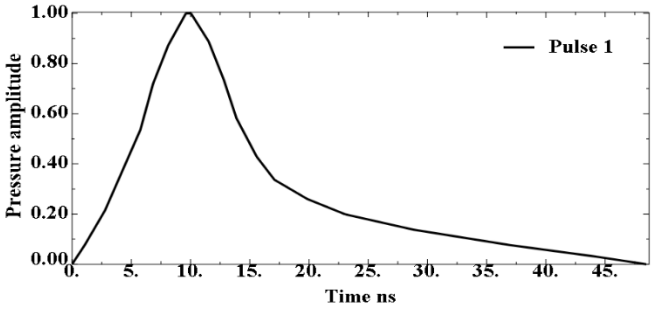


Figure 5. Temporal profile of pressure for a laser with FWHM of 10ns, pulse energy of 3J and wave length of 1064nm.

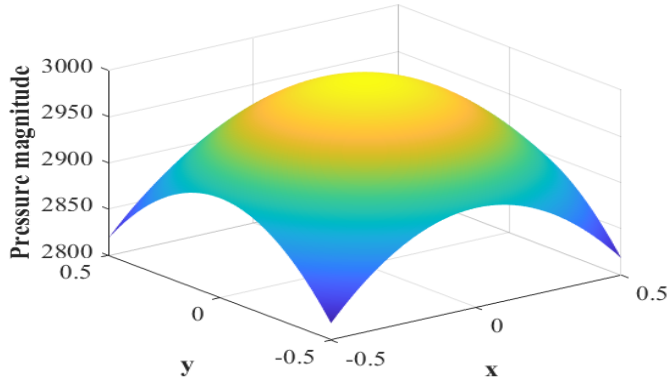


Figure 6. Gaussian spatial distribution of pressure.

A 2D axisymmetric computational domain (Figure 7) is set up in ABAQUS to simulate the material deformation under the surface pressure load [1,2,3]. It is useful to study the effect of multi-pulse shooting on the same spot. Since the affected area is very small compared to the size of the workpiece, only a small part of the workpiece is modeled. CAX4R (4-node bilinear axisymmetric quadrilateral, reduced integration and hourglass control) elements are used for finite computational domain. Infinite elements (CINAX4) are used to provide quiet boundaries around the finite domain. The size of finite domain is chosen such that the residual stress profile is not affected by the further increase in size of the domain. The size of the mesh is chosen based on mesh sensitivity analysis. Mesh sensitivity analysis is decreasing the size of the mesh till the results become consistent.

A user subroutine *VDLOAD is used to model temporal and spatial variation of pressure on the sample surface [7, 16, 18, 19]. ABAQUS/Explicit algorithm is used to obtain the dynamic material response. The workpiece is subjected to the shooting of four laser pulses at the same location with different repetition rates. For lower repetition rates where there is no overlap of pressure pulses, each pressure pulse is given in a step with step time equal to repetition rate. At high repetition rates where there is temporal overlap between pressure pulses, the overlapping pressure pulses are specified in a single step. The overlap of pressure pulses is specified using amplitude definition, based on the assumption that the consequence pressure pulses have linear superposition.

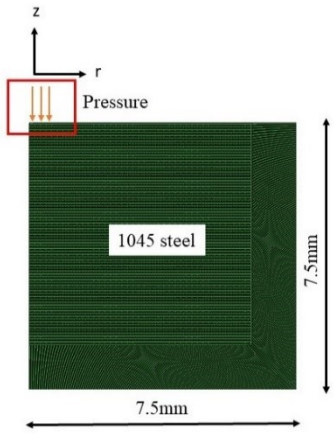


Figure 7. Axe-symmetric model set up for 1mm spot diameter.

In LSP, the material is strained at high rates exceeding 106 s-1. At this high strain rate, the yield strength and elastic modulus of the material change. Hence, a model which accurately captures the elastic-plastic material behavior is required. Amarchinta et al. has compared elastic perfectly plastic (EPP) model, Zerilli-Armstrong (ZA) Model and Johnson-Cook (JC) model in [20] and concluded that the results from JC model are consistent with experimental results. Hence, the elastic-plastic behavior of 1045 steel is modeled using JC equation [2,4,7,13,15,17,19,20,21,22,23,24,25]. The flow stress is calculated as a product of strain hardening term, strain rate dependent term and temperature term [19]. Because of the short time scale, the process is considered as adiabatic and the temperature term is neglected. The equation is given as

$$\sigma = [\, A + B\varepsilon^{n} \,][1 + C \ln \frac{\dot{\varepsilon}}{\dot{\varepsilon}_0}\,][1 - T^{m}\,] \qquad (2)$$

where σ is flow stress, ε is strain, $\dot{\varepsilon}$ is strain rate, A is yield stress, B is work hardening modulus, n is work hardening coefficient and C is strain rate sensitivity. The material constants A, B, C and n need to be determined experimentally. The constants for 1045 steel are shown in Table 1 [17,24].

Table 1. Material properties of 1045 steel [17, 24]

| Properties | Value |
|---|---|
| Density | 7580 kg/m$^3$ |
| Youngs modulus | 206GPa |
| Poisson's ratio | 0.3 |
| A | 507MPa |
| B | 320MPa |
| C | 0.064 |
| n | 0.28 |

## 5. RESULTS AND DISCUSSION

### 5.1 Benchmark simulation

To validate the numerical model in the current research, a 2D model is replicated using parameters in [3]. The surface stress profile in r direction for a mesh density of 0.5 are compared with FEA data and experimental data from Ref. 3. Figure 8 shows that the developed model is consistent with the numerical model from the literature. The small differences in the residual stress values are attributed to the missing simulation setup parameters like size of time increment and total step time of implicit process.

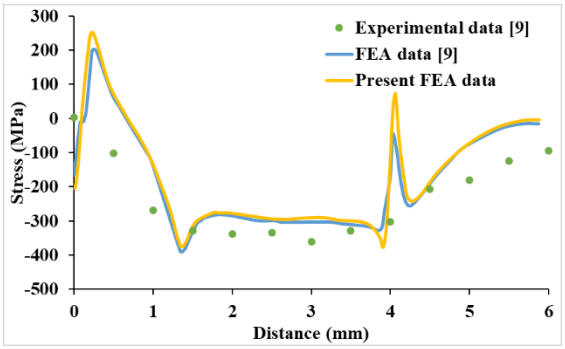


Figure 8: Surface stress profile from benchmark simulation

### 5.2 Effect of repetition rate

The surface (along r) and in-depth (along z) distributions (Figure 9) of residual stresses are compared at different repetition rates for a spot of diameter 0.1 mm. Figure 10 shows that repetition rates below 10 MHz do not have significant impact on in-depth stress distributions. High residual stresses of 820 MPa are induced to a greater depth at high repetition rate of 100 MHz. This is because of the increase in amplitude of the pressure due to overlapping laser pulses at 100 MHz. Figure 11 shows that the surface stress profiles remain unaffected for repetition rates lower than 10 MHz. At high repetition rate of 100 MHz, the surface stresses become tensile (600 MPa). This is attributed to the increase in relaxation of surface residual stress due to free degree of freedom in z direction with increase in pressure magnitude (for constant spot size).

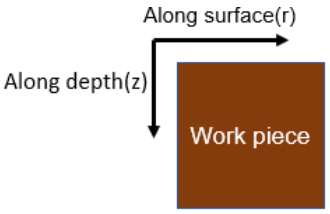


Figure 9. Illustration of surface and in-depth directions

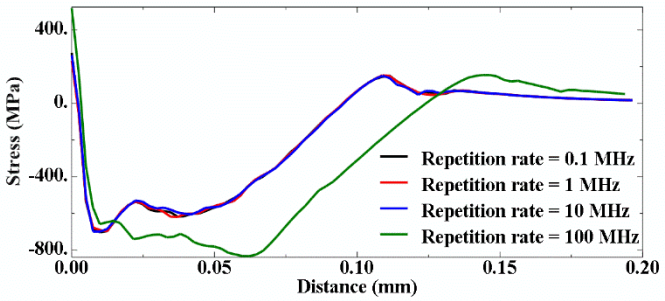


Figure 10. Comparing in-depth residual stress distributions at repetition rates of 0.1MHz, 1MHz, 10MHz and 100MHz for a spot diameter of 0.1mm.

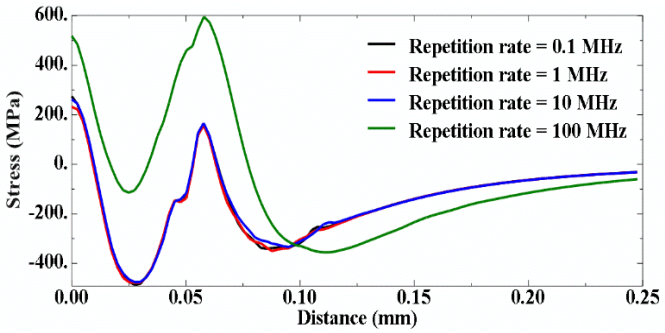


Figure 11. Comparing surface residual stress distributions at repetition rates of 0.1MHz, 1MHz, 10MHz and 100MHz for a spot diameter of 0.1mm.

The effect of repetition rates between 10 MHz-100 MHz and after 100 MHz are studied, considering the rapid increase in peak value and affected depth of compressive stress from 10 MHz to 100 MHz. Figures 12 and 13 shows the variation of in-depth and surface stress profiles between repetition rates from 10 MHz to 200 MHz. For repetition rate of 20 MHz, there is no time for relaxation between consecutive pressure pulses and for repetition rate of 33.3 MHz, the overlap between successive pressure pulses does not change the peak pressure and the peak compressive stress. At the repetition rates of 20 MHz and 33.3 MHz, the peak compressive stress is constant but the plastically affected depth decreases compared with the repetition rate of 10 MHz. This is due to decrease in the depth travelled by the incoming pressure wave because of the effect of active relaxation

waves in depth (z) direction. The depth and peak compressive stress increase with the increase in repetition rates after 100 MHz due to the increase in peak magnitude of pressure by pulse superposition.

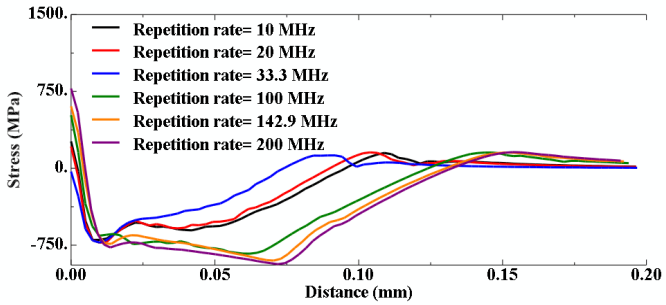


Figure 12. Comparing in-depth residual stress distributions at repetition rates of 33.3MHz, 50MHz, 10MHz and 100MHz for a spot diameter of 0.1mm.

As shown in Figure 13, the peak surface tensile stress at the center decreases between repetition rates of 10 MHz and 100 MHz, and then increases after 100 MHz. The tensile stress at the center increases with the increase in peak pressure magnitude. For repetition rates of 20 MHz and 33.3 MHz, the peak magnitude remains the same as the magnitude at 10 MHz but there is no time interval between successive pulses. The continuous pressure pulse decreases the effect of relaxation waves at the center.

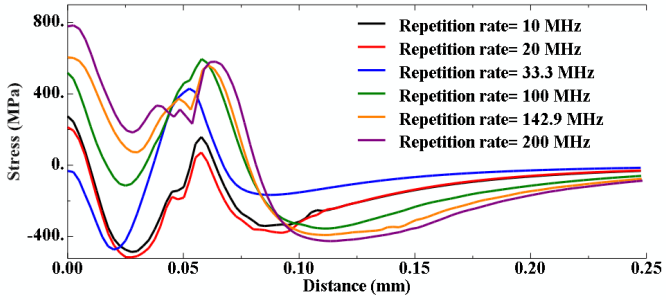


Figure 13. Comparing surface residual stress distributions at repetition rates of 33.3MHz, 50MHz, 10MHz and 100MHz for a spot diameter of 0.1mm.

The spot diameter is increased to 1mm to study the effect of repetition rate at larger diameters of the pulse. Figure 14 and Figure 15 show the variation of in-depth and surface stress profiles at various repetition rates for spot diameter of 1 mm. The compressive stress and plastically affected depth are not significantly affected by repetition rates below 10 MHz. At high repetition rate of 100 MHz, the peak compressive stress and plastically affected depth increases abruptly because of the increase in peak magnitude of pressure due to overlapping laser pulses. Surface tensile stresses are absent for larger spots because the strength of the relaxation waves is not sufficient to cause significant reverse straining at repetition rates below 10 MHz. However, at high repetition rate of 100 MHz, the overlapping pressure pulses generate strong relaxation waves which cause tensile stresses at the center of spot.

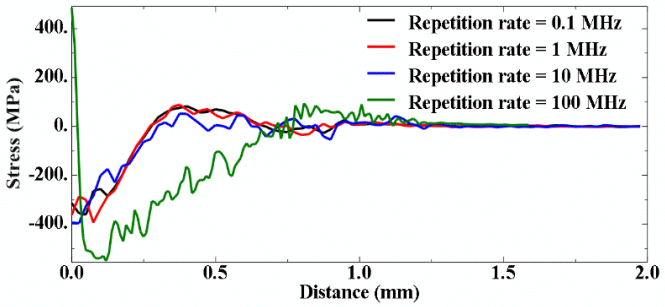


Figure 14. Comparing in-depth residual stress distributions at repetition rates of 0.1MHz, 1MHz, 10MHz and 100MHz for a spot diameter of 1mm.

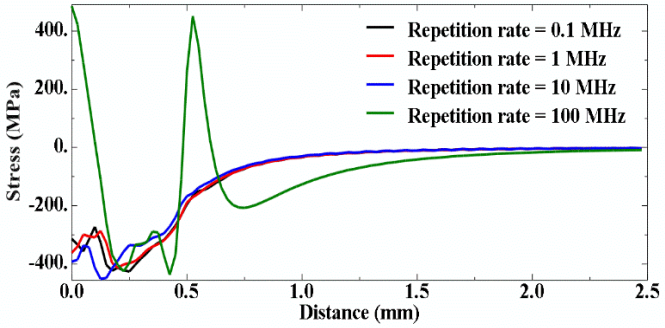


Figure 15. Comparing surface residual stress distributions at repetition rates of 0.1MHz, 1MHz, 10MHz and 100MHz for a spot diameter of 1mm.

The diameter of the spot is decreased to 0.01 mm to study the effect of repetition rate for smaller laser pulses. Figure 16 and Figure 17 shows the variation of in-depth and surface stress profiles at various repetition rates for spot diameter of 0.01 mm. There is no significant effect of repetition rates below 10 MHz on stress profiles. The peak compressive stress and plastically affected depth are high at high repetition rate of 100 MHz due to overlapping of the pressure pulses. The surface stresses are tensile from r/2 for all repetition rates. The reverse straining has the dominant effect at the boundary of the spot instead of center because of the very small size of the affected area. However, the reverse straining decreases at high repetition rate of 100 MHz. Due to overlapping pressure pulses at 100 MHz and very small size of the spot, the metal is highly deformed affecting the metal outside the spot boundary (600 MPa residual stress outside the spot boundary).

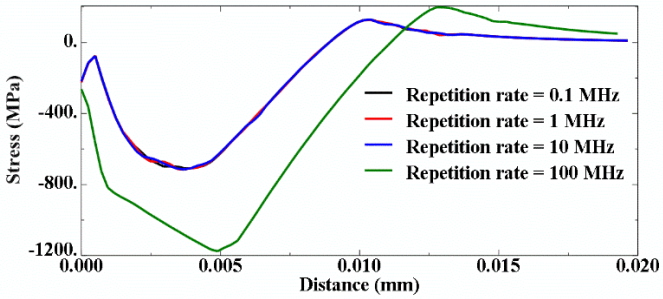


Figure 16. Comparing in-depth residual stress distributions at repetition rates of 0.1MHz, 1MHz, 10MHz and 100MHz for a spot diameter of 0.01mm.

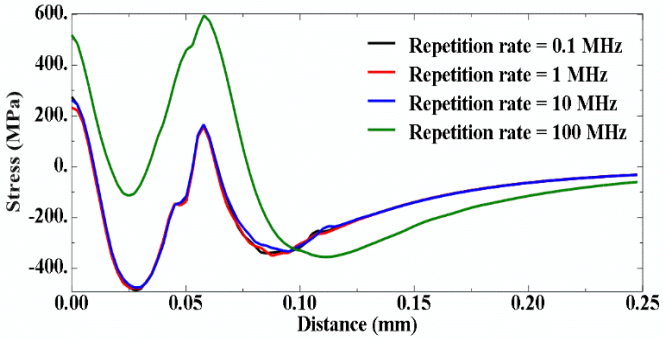


Figure 17. Comparing surface residual stress distributions at repetition rates of 0.1MHz, 1MHz, 10MHz and 100MHz for a spot diameter of 0.01mm.

### 5.3 Effect of spot size at constant repetition rates

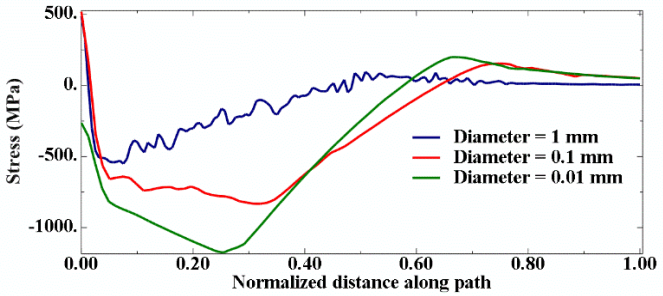


Figure 18. Comparing in-depth residual stress distributions at repetition rate of 100MHz for a spot diameter of 1mm, 0.1mm, 0.01mm.

The effect of spot size is studied at constant repetition rate to understand the variation of peak compressive stresses. The stress profiles for different spot sizes are plotted along normalized distance. The normalized distance is defined as the ratio of true distance at point to the total distance of the path. Figure 18 shows the variation of in-depth profiles with spot size at constant repetition rate of 100 MHz. It should be noticed that the peak laser-induced shock wave is kept the same for all laser diameters. The peak compressive stress is high for small spot diameter of 0.01 mm. With increase in spot size, the peak compressive stress decreases due to planar relaxation of the shock wave. Therefore, small beam diameter is beneficial to induced higher compressive residual stress, but it will be slower to treat large surfaces.

## 6. CONCLUSION

In this study, the effects of repetition rate, spot size, and scanning pattern of LSP are investigated by numerical analysis. It is revealed that at low repetition rates, where the interval between successive pulses is longer than the material relaxation time, the effect of repetition rate on residual stress distribution is negligible. For repetition rates with less overlap between successive pulses, the peak compressive stress remains the same as the value at lower repetition rates, but the plastically affected depth decreases because of the interaction between the relaxation wave and the incoming pressure pulse. At very high repetition rates (>100 MHz), where the time interval between successive pulses is even shorter than the shock duration, the interaction of metal with shock wave is significantly different, leading to a different residual stress profile. Stronger residual stress with deeper distribution are obtained compared with lower repetition rate cases.

The effect of repetition rate on the residual stress in-depth distribution at different spot sizes is also studied. Deeper distributions with high residual stress are obtained at different spot sizes at high repetition rates. However, the peak compressive stress decreases with increase in spot size. At lower repetition rate, the surface tensile residual stresses are high for smaller spot size. At very high repetition rates, due to stronger pressures acting on very small area, the surface tensile stresses for smaller spot decreases and high compressive stresses are induced outside the spot boundary.

## ACKNOWLEDGEMENTS

The authors wish to gratefully acknowledge the financial support provided for this study by the National Science Foundation (Grant No: 1762581-CMMI) and the computational support provided by Palmetto Cluster in Clemson University.

## REFERENCES

[1] Braisted, W., & Brockman, R. (1999). Finite element simulation of laser shock peening. *International Journal of Fatigue*, *21*(7), 719-724.

[2] Peyre, P., Sollier, A., Chaieb, I., Berthe, L., Bartnicki, E., Braham, C., & Fabbro, R. (2003). FEM simulation of residual stresses induced by laser peening. *The European Physical Journal-Applied Physics*, *23*(2), 83-88.

[3] Ding, K., & Ye, L. (2006). Simulation of multiple laser shock peening of a 35CD4 steel alloy. *Journal of Materials Processing Technology*, *178*(1-3), 162-169.

[4] Singh, G., Grandhi, R. V., & Stargel, D. S. (2011). Modeling and parameter design of a laser shock peening process. *International Journal for*

*Computational Methods in Engineering Science and Mechanics*, *12*(5), 233-253.

[5] Hu, Y., Gong, C., Yao, Z., & Hu, J. (2009). Investigation on the non-homogeneity of residual stress field induced by laser shock peening. *Surface and Coatings Technology*, *203*(23), 3503-3508.

[6] Peyre, P., & Fabbro, R. (1995). Laser shock processing: a review of the physics and applications. *Optical and quantum electronics*, *27*(12), 1213-1229.

[7] Peyre, P., Hfaiedh, N., Song, H., Ji, V., Vignal, V., Seiler, W., & Branly, S. (2011). Laser shock processing with two different laser sources on 2050-T8 aluminum alloy. *International Journal of Structural Integrity*, *2*(1), 87-100.

[8] Ding, K. (2003). Three-dimensional dynamic finite element analysis of multiple laser shock peening processes. *Surface Engineering*, *19*(5), 351-358.

[9] Wei, X. L., & Ling, X. (2014). Numerical modeling of residual stress induced by laser shock processing. *Applied Surface Science*, *301*, 557-563.

[10] Hu, Y., Yao, Z., & Hu, J. (2006). 3-D FEM simulation of laser shock processing. *Surface and Coatings Technology*, *201*(3-4), 1426-1435.

[11] Achintha, M., & Nowell, D. (2011). Eigenstrain modelling of residual stresses generated by laser shock peening. *Journal of Materials Processing Technology*, *211*(6), 1091-1101.

[12] Wu, B., Tao, S., & Lei, S. (2010). Numerical modeling of laser shock peening with femtosecond laser pulses and comparisons to experiments. *Applied Surface Science*, *256*(13), 4376-4382.

[13] Julan, E., Stolz, C., Taheri, S., Peyre, P., & Gilles, P. (2013). Simulation of laser peening for generation of a surface compressive stresses. In *21st Congress French Mechanics, Bordeaux, France, Aug* (pp. 26-30).

[14] Luo, K. Y., Lu, J. Z., Wang, Q. W., Luo, M., Qi, H., & Zhou, J. Z. (2013). Residual stress distribution of Ti-6Al-4V alloy under different ns-LSP processing parameters. *Applied Surface Science*, *285*, 607-615.

[15] Hfaiedh, N., Peyre, P., Song, H., Popa, I., Ji, V., & Vignal, V. (2015). Finite element analysis of laser shock peening of 2050-T8 aluminum alloy. *International Journal of Fatigue*, *70*, 480-489.

[16] Guo, Y. B. (2011). Laser shock peening: modeling, simulations, and applications. In *Numerical Simulations-Applications, Examples and Theory*. InTech.

[17] Hu, Y., & Yao, Z. (2008). Numerical simulation and experimentation of overlapping laser shock processing with symmetry cell. *International Journal of Machine Tools and Manufacture*, *48*(2), 152-162.

[18] Warren, A. W., Guo, Y. B., & Chen, S. C. (2008). Massive parallel laser shock peening: simulation, analysis, and validation. *International Journal of Fatigue*, *30*(1), 188-197.

[19] Voothaluru, R., & Liu, C. R. (2010, January). Finite Element Analysis of the Effect of Overlapping Impacts of Laser Shock Peening Within Annealed AISI 1053 Steel. In *ASME 2010 International Manufacturing Science and Engineering Conference* (pp. 221-228). American Society of Mechanical Engineers.

[20] Amarchinta, H. K., Grandhi, R. V., Langer, K., & Stargel, D. S. (2008). Material model validation for laser shock peening process simulation. *Modelling and simulation in materials science and engineering*, *17*(1), 015010.

[21] Peyre, P., Chaieb, I., & Braham, C. (2007). FEM calculation of residual stresses induced by laser shock processing in stainless steels. *Modelling and simulation in materials science and engineering*, *15*(3), 205.

[22] Brockman, R. A., Braisted, W. R., Olson, S. E., Tenaglia, R. D., Clauer, A. H., Langer, K., & Shepard, M. J. (2012). Prediction and characterization of residual stresses from laser shock peening. *International Journal of Fatigue*, *36*(1), 96-108.

[23] Correa, C., Peral, D., Porro, J. A., Díaz, M., de Lara, L. R., García-Beltrán, A., & Ocaña, J. L. (2015). Random-type scanning patterns in laser shock peening without absorbing coating in 2024-T351 Al alloy: a solution to reduce residual stress anisotropy. *Optics & Laser Technology*, *73*, 179-187.

[24] Hu, Y., & Yao, Z. (2008). Overlapping rate effect on laser shock processing of 1045 steel by small spots with Nd: YAG pulsed laser. *Surface and Coatings Technology*, *202*(8), 1517-1525.

[25] Wu, X., Huang, C., Wang, X., & Song, H. (2011). A new effective method to estimate the effect of laser shock peening. *International Journal of Impact Engineering*, *38*(5), 322-329.